Vol. 32, No. 4 Journal of Semiconductors April 2011

Design and fabrication of a MEMS Lamb wave device based on ZnO thin film*

Liu Mengwei(刘梦伟)†, Li Junhong(李俊红), Ma Jun(马军), and Wang Chenghao(汪承灏)

Institute of Acoustics, Chinese Academy of Sciences, Beijing 100190, China

Abstract: This paper presents the design and fabrication of a Lamb wave device based on ZnO piezoelectric film. The Lamb waves were respectively launched and received by both Al interdigital transducers. In order to reduce the stress of the thin membrane, the ZnO/Al/LTO/Si_3N_4/Si multilayered thin plate was designed and fabricated. A novel method to obtain the piezoelectric constant of the ZnO film was used. The experimental results for characterizing the wave propagation modes and their frequencies of the Lamb wave device indicated that the measured center frequency of antisymmetric A_0 and symmetric S_0 modes Lamb wave agree with the theoretical predictions. The mass sensitivity of the MEMS Lamb wave device was also characterized for gravimetric sensing application.

Key words: Lamb wave; MEMS; ZnO film; composite plate

DOI: 10.1088/1674-4926/32/4/044006 **EEACC:** 2860

1. Introduction

MEMS Lamb wave devices have been explored as gas chemical sensors[1, 2], biological sensors[3, 4], pressure sensors[5, 6], resonators[7, 8], micro pumps[9], particle transfer devices[10], and so on. These Lamb wave devices have several advantages: higher sensitivity due to the flexural mode Lamb wave operating at the micrometer scale thin plate; easy integration with IC; the capability to operate in an aqueous environment of flexural mode Lamb wave device because of its less propagating velocity than the velocity of sound in the neighboring fluid; and environmental isolation of the interdigital electrodes located at the piezoelectric composite plate and exposing only the backside of the plate as the operating side[11−13].

Lamb waves are usually excited and detected by both interdigital transducers on a thin piezoelectric composite plate. ZnO, AlN and PZT thin films are the three primary piezoelectric materials used in piezoelectric MEMS devices. PZT has the highest piezoelectric constant and electromechanical coupling coefficient. However, PZT films have higher acoustic wave attenuation and lower sound velocities. Although AlN films have a much higher phase velocity and chemical stability compared to ZnO films, they have lower piezoelectric coupling and more difficulties in deposition and texture control. ZnO films have been widely used in MEMS Lamb devices for chemical and biological sensors[2, 4]. However, the in-plane stress of ZnO film developing during the fabrication process affects the phase velocity and properties, and even destroys the membrane structures and reduces the yield and life-time of the MEMS Lamb wave device. In this paper, in order to reduce the stress of the thin membrane, the Lamb wave device is fabricated using the ZnO/Al/LTO/Si_3N_4/Si multilayered thin plate. ZnO films with c-axis orientation are deposited by an RF magnetron sputtering technique. It is difficult to measure the piezoelectric constant of films because they are very thin and always clamped to substrates[14]. A novel untouched method to obtain the piezoelectric constant of the ZnO film is used in this paper. The detailed design, fabrication procedure, and some performance of the Lamb wave device are presented. The mass sensitivity of the MEMS Lamb wave device is also characterized for gravimetric sensing application.

2. Design

In MEMS Lamb wave device applications, the lowest order antisymmetric A_0 and symmetric S_0 modes in plates with a small thickness-to-wavelength ratio are the two most useful ones. Here, the thin plate may be considered approximately as a homogeneous, isotropic plate. The approximate analytical expressions of Lamb wave velocities are[15] as follows.

For A_0 mode,

$$V_\mathrm{p} = \frac{2\pi h}{\lambda}\sqrt{\frac{E}{12(1-\nu^2)\rho}}\frac{1}{\sqrt{\dfrac{\pi^2 h^2}{3\lambda^2}+1}}. \tag{1}$$

For S_0 mode,

$$V_\mathrm{p} = \sqrt{\frac{E}{(1-\nu^2)\rho}}, \tag{2}$$

where E, ν, ρ and h are Young's modulus, Poisson's ratio, density, and thickness of the thin plate, respectively, and λ represents the wavelength of the Lamb wave. In very thin plates, the velocity of the S_0 mode Lamb wave is dispersionless, and no dependence on the thickness, while the wave velocity of A_0 mode increases with the thickness.

The center frequency of the Lamb device is equal to

$$f_0 = \frac{V_\mathrm{p}}{\lambda}. \tag{3}$$

Therefore, based on Eq. (1) (or Eqs. (2)) and (3), the interdigital transducer structure and the plate thickness can be designed according to the device required center frequency. In

---

* Project supported by the National Natural Science Foundation of China (No. 10804119).

† Corresponding author. Email: liumw@mail.ioa.ac.cn

Received 30 September 2010, revised manuscript received 6 December 2010

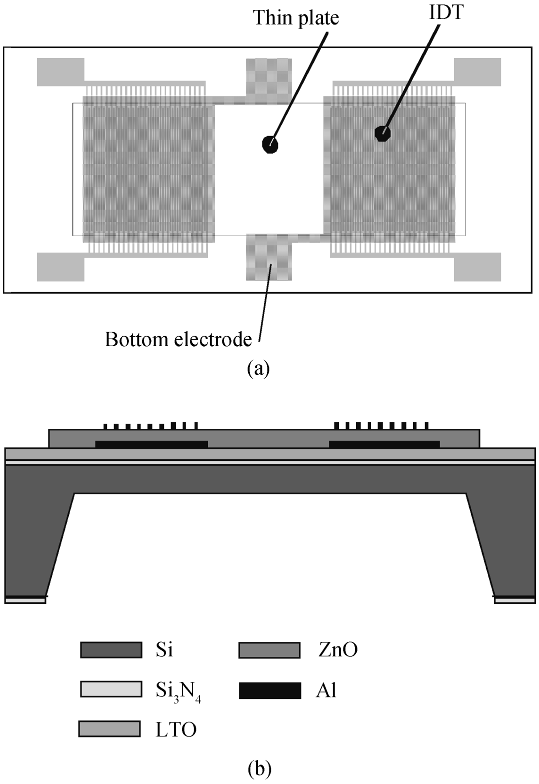

Fig. 1. Schematic of (a) top view and (b) cross-sectional view of the Lamb wave device.

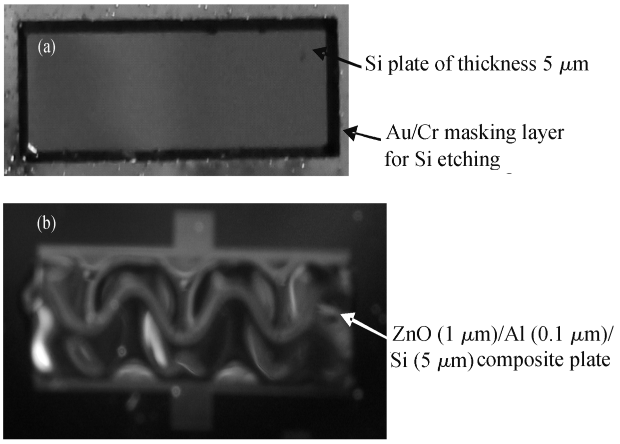

Fig. 2. (a) Back-side photograph of the 5 μm thick Si plate. (b) Front-side photograph of the ZnO (1 μm)/Al (0.1 μm)/Si (5 μm) piezoelectric composite plate.

Table 1. Material parameters of the ZnO/Al/LTO/Si_3N_4/Si multilayered plate[17, 18].

Material	Thickness (μm)	Young's modulus, E (GPa)	Poisson's ratio υ	Density, ρ (kg/m^3)
Si	14	162	0.27	2320
Si_3N_4	0.5	146	0.25	3000
LTO	2	73	0.17	2660
ZnO	1	120	0.446	5610

this study, the Lamb waves were respectively launched and received by both Al IDTs deposited on a ZnO/Al/LTO/Si_3N_4/Si thin plate, as shown in Fig. 1. The design of the two IDTs is described as follows. The acoustic aperture and pathlength of the Lamb wave transducers are 2.5 and 5.6 mm, respectively. The input and output IDTs of the Lamb device are both constructed by 25 pairs of Al fingers. The width and pitch of the Al electrodes both equal 25 μm, so that the interdigital period, i.e. the wavelength, equals 100 μm. The dimensions of the final suspended thin plate are 9×3 mm^2.

Equation (1) indicates that the phase velocity of the A_0 mode Lamb wave (i.e. flexural plate mode wave, FPW) is related to the thickness of the thin plate. The FPW mass sensitivity for chemical and biological sensing applications is inversely proportional to the plate thickness[16]. However, it is difficult to fabricate the thin and fragile membrane structures due to the stress of the piezoelectric composite plate, which is induced mainly by the in-plane compressive stress of ZnO film developing during the fabrication process. Figure 2 shows the influence of stress in ZnO film. A 5 μm thick Si plate is formed by KOH wet etching substrate of the silicon-on-insulator (SOI) wafer, which has a 5 μm thick Si bonded to a 1 μm thick layer of SiO_2. The SiO_2 layer is removed using the buffered hydrofluoric acid. As shown in Fig. 2(a), the Si plate is flat. However, after a 0.1 μm thick Al film and a 1 μm thick ZnO film are deposited on the Si plate, wrinkles arise on the composite plate, as shown in Fig. 2(b). In this paper, the LTO/Si_3N_4/Si multilayered substrate was designed. A low stress LPCVD (low-pressure chemical vapor deposition) Si_3N_4 layer of thickness 0.5 μm provides electrical isolation for the Lamb device and serves as a mask layer for Si etching. A PECVD (plasma-enhanced chemical vapor deposition) low temperature oxide (LTO) layer of thickness 2 μm compensates the tensile nature of the nitride layer. A Si layer of 14 μm thickness serves as the supporting layer of the thin plate to prevent deformation and to improve yield and life-time of the MEMS Lamb wave device. Table 1 shows the material and thickness parameters of the ZnO/LTO/Si_3N_4/Si multilayered composite plate.

3. Fabrication

The MEMS Lamb device was fabricated using bulk silicon micromachining techniques. The main processing steps are shown in Fig. 3, as follows:

(a) A (100) n-type, double side polished silicon wafer with 300 μm thickness was prepared. After a RCA clean, 0.5 μm LPCVD Si_3N_4 and 2 μm PECVD LTO was deposited on the wafer.

(b) A 140 nm thick Al layer was deposited onto LTO/Si_3N_4 layers by an ion beam method to form a ground plane of the Lamb device. The Al thin layer was patterned by H_3PO_4.

(c) A 1 μm thick high-quality c-axis orientation ZnO piezoelectric layer was deposited on the Al ground plane by RF planar magnetron sputter under the following conditions: 0.5 Pa of Ar/O_2 (2 : 1) gas mixture, 100 W RF power, and 200 ℃ substrate temperature.

(d) The ZnO film was patterned by the wet etching method (4% H_3PO_4 : 96% H_2O) to open up the contact holes for the bottom electrode. A 140 nm thick Al layer was conducted of the IDT electrodes deposited by the ion beam method and pat-

(a) Deposition of Si_3N_4 and LTO

(b) Deposition and pattern of Al bottom electrode

(c) Deposition and pattern of ZnO

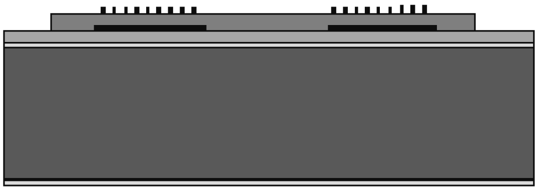

(d) Deposition and pattern of Al IDT electrodes

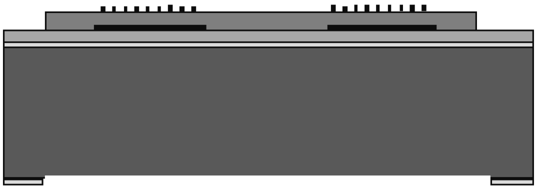

(e) Pattern of backside Si_3N_4 film

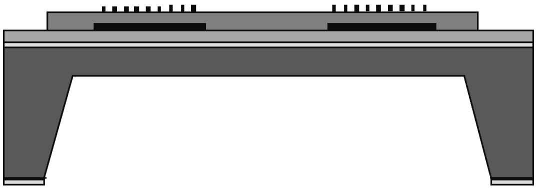

(f) Wet etching of bulk-Si

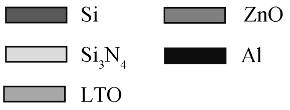

Fig. 3. Fabrication procedure of the Lamb wave device.

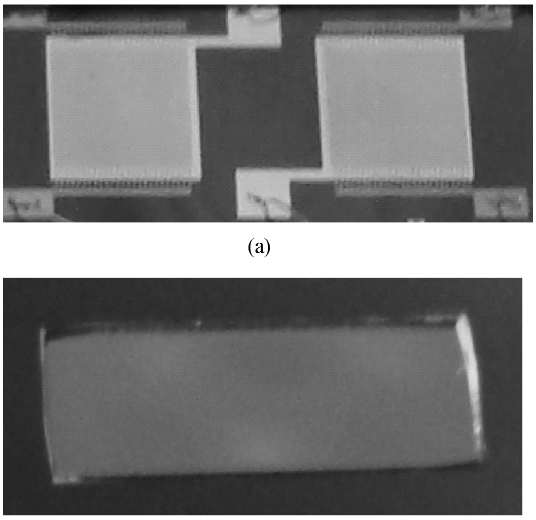

(a)

(b)

Fig. 4. (a) Front-side and (b) back-side photographs of the Lamb wave device.

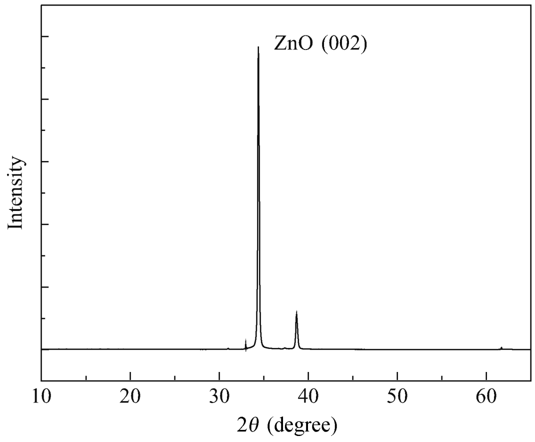

Fig. 5. XRD pattern of the ZnO film.

terned by the lift-off photolithographic method.

(e) After a double side alignment process, the backside Si_3N_4 layer was patterned by the ICP (inductively coupled plasma) process to open up the etching windows.

(f) Finally, the silicon substrate was etched in 30 wt%, 95 ℃ KOH anisotropic etching solution. During etching in KOH solution, the wafer was loaded in a Teflon jig to protect the front-side from the etchant. The silicon etching rate is 2.3 μm/min. After the structure releasing process, the free-standing floating plate with ZnO (1 μm)/LTO (2 μm)/Si_3N_4 (0.5 μm)/Si (14 μm) was formed. Figure 4 shows the front-side and back-side photographs of the Lamb wave device.

4. Measured results and discussion

The crystalline structure and orientation of the ZnO film was examined by X-ray diffraction, as shown in Fig. 5. The ZnO film grows with a high degree of (002) orientation. The XRD pattern indicates that the deposited ZnO film is a highly c-axis oriented piezoelectric film. The SEM photographs of the ZnO thin film surface indicate that the film is dense, as shown in Fig. 6. The average grain size of the ZnO films is about 200–300 nm.

The dielectric constant ε_r and piezoelectric constant g_{31} are two important parameters of the piezoelectric film. The dielectric constant ε_r of 10.3 was derived by the measured capacitance of the ZnO film. It is difficult to measure the piezoelectric constant of films because they are very thin and always

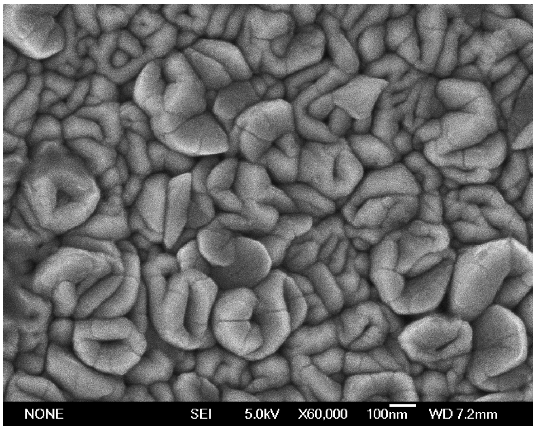

Fig. 6. SEM surface view of the ZnO film.

clamped to substrates. In this paper, the piezoelectric constant g_{31} of the ZnO film was extracted from the sensitivity of the fabricated piezoelectric microphone using this ZnO film.

The characteristics of this method can be described as follows: (1) the applied acoustic pressure is uniform and untouched to the thin piezoelectric membrane structure, which prevents the film from damage; (2) because the piezoelectric microphone is measured far from the resonator frequency, the sensitivity is independent on the frequency.

The sensitivity equation for the piezoelectric microphone with a circular diaphragm is[19]

$$S_{\mathrm{M}} = -\frac{h\left(\dfrac{2\sum h_i - h}{2} - z^0\right)}{T}\frac{E}{1-\nu}g_{31}, \tag{4}$$

where h, E, ν and h are the thickness, Young's modulus and Poisson's ratio of the ZnO film, respectively. $\sum h_i$ and z^0 represent the total thickness and distance from the neutral plane to bottom plane of the composite membrane structure. T is the tension of the microphone.

The measured sensitivity of the piezoelectric microphone with a ZnO (1 μm)/Si_3N_4 (0.5 μm)/LTO (0.2 μm)/Si_3N_4 (0.5 μm) composite circular membrane structure is about –70 dB (1 V/Pa)[17]. The tension of the micromachined composite piezoelectric membrane is about 10 MPa. According to Eq. (4), the piezoelectric constant g_{31} of the ZnO film is –0.045 V·m/N, which is slightly lower than that of ZnO bulk material of –0.049 V·m/N[20].

The transfer characteristics of the Lamb wave delay lines were measured by using an Agilent E5071C network analyzer. Figure 7 shows the frequency response of the S_{21} parameter (insertion loss). In our experiment, the A_0 and S_0 modes are the only two modes which can propagate in the plate at frequency up to 100 MHz. This is because the plate of 17.5 μm thick is much smaller than the acoustic wavelength of 100 μm. The center frequency of the Lamb device f_0 was determined by observing the minimal insertion loss. Figures 6(b) and 6(c) show that the center frequency of the A_0 and S_0 modes Lamb wave device are 21.6 MHz and 77.8 MHz. According to the relationship of Eq. (3), the phase velocities of the two modes are 2160 m/s and 7780 m/s, respectively.

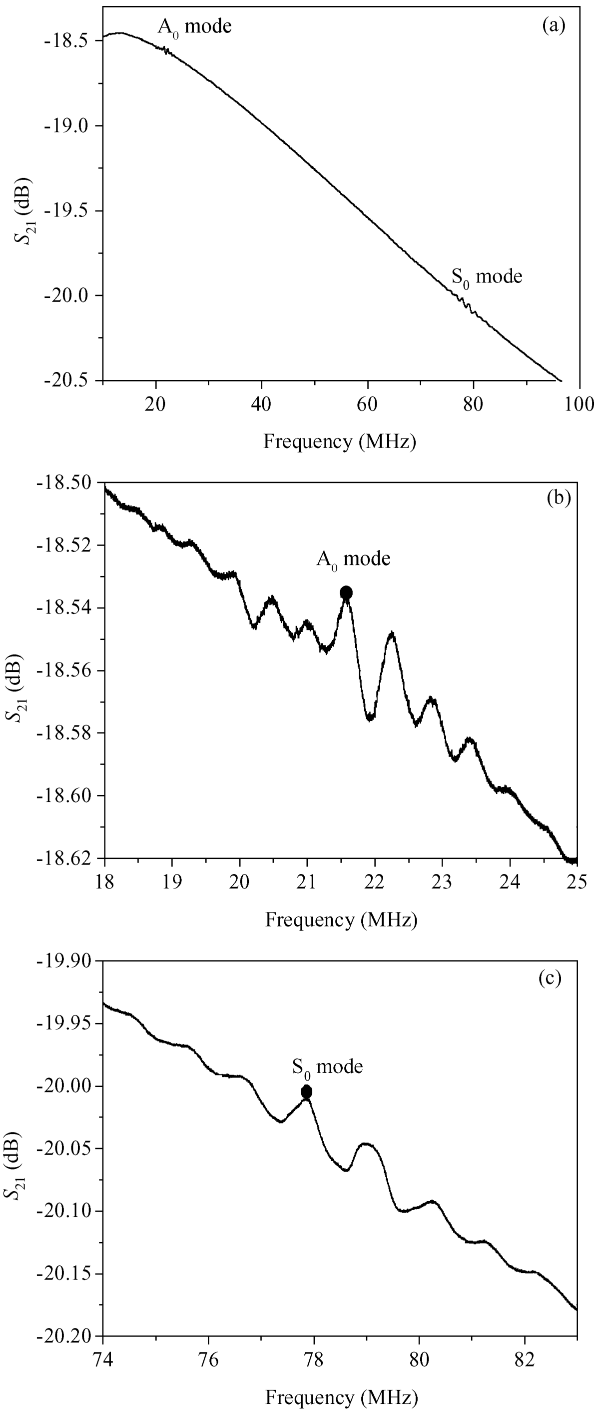

Fig. 7. Frequency response of the fabricated Lamb wave device.

According to Eqs. (1)–(3), the theoretical center frequency of the A_0 and S_0 modes for homogeneous, isotropic plates can be written as

$$f_0 = \frac{2\pi h}{\lambda^2}\sqrt{\frac{E}{12(1-\nu^2)\rho}}\frac{1}{\sqrt{\dfrac{\pi^2 h^2}{3\lambda^2}+1}}, \tag{5}$$

and

$$f_0 = \frac{1}{\lambda}\sqrt{\frac{E}{(1-\nu^2)\rho}}. \tag{6}$$

At the approximate analysis, since the thickness of the Si (14 μm) accounts for 80% of the total thickness of the

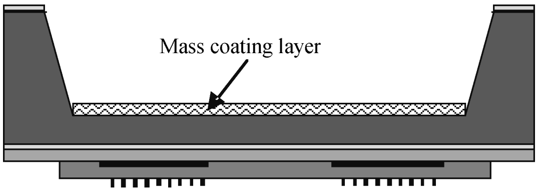

Fig. 8. Measurement method for gravimetric sensing application.

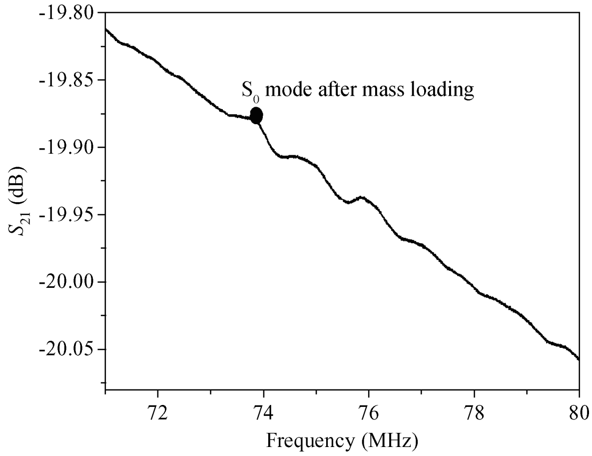

Fig. 9. Frequency response for the S_0 mode of the MEMS Lamb wave device with a mass coating layer of 1 μm thick ZnO film.

fabricated Lamb wave device (17.5 μm), the theoretical center frequency can be estimated by a 17.5 μm thick Si plate. Here, the calculated center frequencies of the A_0 and S_0 modes are 26.2 MHz and 86.58 MHz, respectively. In addition, the material parameters E, ν and ρ of the thin plate can be estimated depending on the material thickness ratio of the ZnO/LTO/Si_3N_4/Si (1 : 2 : 0.5 : 14) multilayered thin plate. For example, $E = (E_{\text{ZnO}} + 2E_{\text{LTO}} + 0.5E_{\text{Si}_3\text{N}_4} + 14E_{\text{Si}})/17.5$. According to this approximation, the calculated center frequency values are 23.7 MHz and 78.5 MHz for the A_0 and S_0 modes, which agree with the measured results. It is indicated that the approximate theoretical analysis for the homogeneous, isotropic plates can be used for the preliminary design of the MEMS Lamb wave device.

The MEMS Lamb wave device was measured for gravimetric sensing application. The mass loading layer is coated on the backside of the device, thus the interdigital electrodes can be protected due to isolation from the testing environment (see Fig. 8). The mass sensitivity is expressed as $\frac{\Delta f/f_0}{\Delta m}$, where Δf is the frequency shift and Δm is the added mass per unit area. In our experiment, ZnO film was used as the mass loading layer. Figure 9 shows the frequency response for the S_0 mode of the MEMS Lamb wave device when 1 μm thick ZnO film was deposited on the Si substrate. The frequency shift due to the mass loading is 4 MHz. The measured mass sensitivity for this type of sensor equals 91.65 cm^2/g. The mass detection resolution should be 0.14 ng/cm^2 when the detectable change in frequency is 1 Hz, which indicates that the MEMS Lamb device has potential applications for the small amount of mass detection of chemical or biological analysis.

5. Conclusion

In this work, a Lamb wave device based on ZnO piezoelectric film was designed and fabricated. The ultrasonic lamb waves were respectively launched and received by both Al interdigital transducers deposited on the ZnO piezoelectric composite plate. In order to reduce stress, the Lamb wave device was fabricated using the ZnO/Al/LTO/Si_3N_4/Si multilayered thin plate. ZnO films with highly (002) preferred orientation was obtained using a RF magnetron sputtering method. A novel method to obtain the piezoelectric constant g_{31} of ZnO film is presented. The MEMS Lamb device was fabricated using bulk silicon micromachining techniques. The experimental results indicate that the approximate theoretical analysis for the homogeneous, isotropic plates can be used for the preliminary design of the MEMS Lamb wave device. Finally, in order to confirm the potential application for the small amount of mass detection, the mass sensitivity of the S_0 mode MEMS Lamb wave device was measured.

Acknowledgement

The authors would like to acknowledge the experimental and theoretical support of Xu Lian and Wei Jianhui.

References

[1] Cunningham B, Weinberg M, Pepper J, et al. Design, fabrication and vapor characterization of a microfabricated flexural plate resonator sensor and application to integrated sensor arrays. Sensors and Actuators B, 2001, 73: 112

[2] Cai Q Y, Park J, Heldsinger D, et al. Vapor recognition with an integrated array of polymer-coated flexural plate wave sensors. Sensors and Actuators B, 2000, 62: 121

[3] Pepper J, Noring R, Klempner M, et al. Detection of proteins and intact microorganisms using microfabricated flexural plate silicon resonator arrays. Sensors and Actuators B, 2003, 96: 565

[4] Huang I Y, Lee M C. Development of a FPW allergy biosensor for human IgE detection by MEMS and cystamine-based SAM technologies. Sensors and Actuators B: Chemical, 2008, 132: 340

[5] Choujaa A, Tirole N, Bonjour C, et al. AlN/silicon Lamb-wave microsensors for pressure and gravimetric measurements. Sensors and Actuators A: Physical, 1995, 46: 179

[6] Duhamel R, Robert L, Jia H, et al. Sensitivity of a Lamb wave sensor with 2 μm AlN membrane. Ultrsonics, 2006, 44: e893

[7] Rinaldi M, Zuniga C, Piazza G. 5–10 GHz AlN contour-mode nanoelectromechanical resonators. IEEE MEMS Symposium, 2009: 916

[8] Lin C M, Yen T T, Lai Y J, et al. Temperature-compensated aluminum nitride lamb wave resonators. IEEE Trans Ultrasonics, Ferroelectrics, and Frequency Control, 2010, 57(3): 524

[9] Black J P, White R M, Grate J W. Microsphere capture and perfusion in microchannels using flexural plate wave structures. Ultrasonic Symposium, 2002: 475

[10] Luginbuhl P, Collins S D, Racine G A, et al. Microfabricated Lamb wave device based on PZT sol–gel thin film for mechanical transport of solid particles and liquids. J Microelectromechan Syst, 1997, 6(4): 337

[11] Grate J W, Wenzel S W, White R M. Flexural plate wave devices for chemical analysis. Analytical Chemistry, 1991, 63: 1552

[12] Cheeke D N, Wang Z. Acoustic wave gas sensors. Sensors and

Actuators B: Chemical, 1999, 59: 146

[13] Vellekoop M J. Acoustic wave sensors and their technology. Ultrasonics, 1998, 36: 7

[14] Liu J M, Pan B, Chan H L W, et al. Piezoelectric coefficient measurement of piezoelectric thin films: an overview. Materials Chemistry and Physics, 2002, 75(1–3): 12

[15] Redwood M R. Mechanical waveguides. Oxford: Pergamon Press, 1960

[16] Wenzel S W, White R M. Analytic comparison of the sensitivities of bulk-wave, surface-wave, and flexural plate-wave ultrasonic gravimetric sensors. Appl Phys Lett, 1989, 54(20): 1976

[17] Kovac G T. Micromachined transducers sourcebook. New York: McGraw-Hill Science, 1998

[18] Fu Y Q, Luo J K, Du X Y, et al. Recent developments on ZnO films for acoustic wave based bio-sensing and microfluidic applications: a review. Sensors and Actuators B: Chemical, 2010, 143: 606

[19] Li Junhong. Piezoelectric films and piezoelectric micromachined transducers. PhD Thesis, Institute of Acoustics, Chinese Academy of Sciences, Beijing, 2009 (in Chinese)

[20] Auld B A. Acoustic field and waves in solids. New York: John Wiley, 1973